

## LIFETIME ENHANCEMENT IN STRING RIBBON SILICON – A STUDY BASED ON SPATIALLY RESOLVED MEASUREMENTS

P. Geiger, G. Kragler, G. Hahn, P. Fath, E. Bucher

Universität Konstanz, Fachbereich Physik, Fach X916, 78457 Konstanz, Germany

Tel.: +49-7531-88-2132, Fax +49-7531-88-3895, e-mail: [patric.geiger@uni-konstanz.de](mailto:patric.geiger@uni-konstanz.de)

**ABSTRACT:** The grain structure of String Ribbon silicon as well as the distribution of structural defects are significantly different from those of standard cast multicrystalline silicon. In order to achieve sufficient cell efficiencies it is necessary to enhance starting lifetimes of minority charge carriers by implementing appropriate cell fabrication processes including for example P- and Al-gettering steps. A further method for lifetime improvement in multicrystalline silicon is the passivation of defects with atomic hydrogen originating from a plasma. This technique as well as the mentioned gettering steps and synergetic effects have been investigated in this study. In contrast to former work of other groups, however, we have used the method of microwave detected photoconductance decay. In this way spatially resolved lifetime mappings have been obtained, an aspect that has proven to be essential for investigating String Ribbon silicon as bulk lifetimes vary strongly in this material. Moreover, regions of comparable as grown lifetimes have been found which react very differently on various processing steps. According to their inhomogeneous distribution these areas influence integral measurements. Furthermore, it turned out that the impact of the applied processing steps depends also partly on the starting lifetime.

Keywords: Ribbon Silicon – 1: Lifetime – 2: Gettering – 3

### 1 INTRODUCTION

String Ribbon silicon is produced by Evergreen Solar Inc. and has just made the step from pilot line to industrial production. Grown directly out of the melt it addresses the problem of wafer costs by avoiding cost intensive wafering steps and related material losses. This growth procedure, however, causes a grain structure and a distribution of structural defects which are significantly different from those in conventional cast multicrystalline silicon. In order to achieve sufficient solar cell efficiencies it is therefore necessary to enhance starting lifetimes of minority charge carriers by implementing appropriate cell fabrication processes. Consequently, the impact of different processing steps on String Ribbon silicon material has to be investigated. Measuring the lifetime of minority charge carriers before and after the application of a processing step is one possibility to do so. Some work in this field has already been done with the help of integral measurements [1, 2]. But as strong variations of material properties within some square centimeters of wafer area have been found earlier, it is not obvious that different regions are affected by the various processing steps in the same way and to the same extent [3]. For that reason we have studied the influence of different processing steps on bulk lifetime in String Ribbon silicon in a spatially resolved way.

### 2 EXPERIMENTAL APPROACH

#### 2.1 Spatially resolved bulk lifetime measurement

Lifetime mappings of String Ribbon samples covering an area of  $5 \cdot 5 \text{ cm}^2$  were realized with the method of microwave detected photoconductance decay. Measurements were performed under low injection conditions and with bias light. The laser used for charge carrier generation had a wavelength of 905 nm. In this way an effective lifetime is obtained that can be calculated from bulk lifetime and sur-

face recombination velocity. By applying a surface passivation the latter one can be neglected so that the system measures the bulk lifetimes  $\tau_{bulk}$ . In this study the wafers' surfaces were passivated by an iodine-alcohol solution. Consequently, the impacts and synergetic effects of different processing steps could be partly investigated on the same sample by measuring the corresponding changes in bulk lifetime with the help of a reproducible surface passivation.

For the determination of  $\tau_{bulk}$  from the decay of photoconductance it is necessary to select an adequate time range in which the decay is evaluated. Due to the strong variations of material quality within String Ribbon wafers, however, it is usually not possible to choose a single time range well-suited for the whole sample. Therefore, generally either rather low or quite high lifetime values represented in  $\mu$ -PCD mappings are not reliable. This problem was addressed by measuring each wafer partly or as a whole several times with different time ranges. The resulting data was finally combined in an adequate way with the help of developed software procedures. As a consequence rather low lifetime values as well as quite high ones are reliable in the mappings shown in this study.

#### 2.2 Design of experiment

Four different processing sequences represented by the four columns shown in Fig. 1 have been investigated. Comparable surfaces of the different wafers were provided by an acid defect etching step, during which  $20 \mu\text{m}$  were removed on each side. In the following the wafers were chemically cleaned and their surfaces were passivated with an iodine-alcohol solution before each  $\mu$ -PCD measurement indicated in the different columns of the schematic drawing. The P-emitter diffusion mentioned in Fig. 1 was performed in a quartz tube furnace and the Aluminium required for gettering was evaporated. Before the subsequent lifetime measurement both, emitter as well as back surface field (BSF), were etched back. In this way problems during measurement possibly caused by recombination in the emitter region or by

an insufficient or at least not comparable surface passivation could be avoided. Hydrogen passivation was realized with the help of a microwave induced remote hydrogen plasma (MIRHP) as described in [4]. Illuminating the samples for ten hours under one sun made it finally possible to examine the passivations' stability.

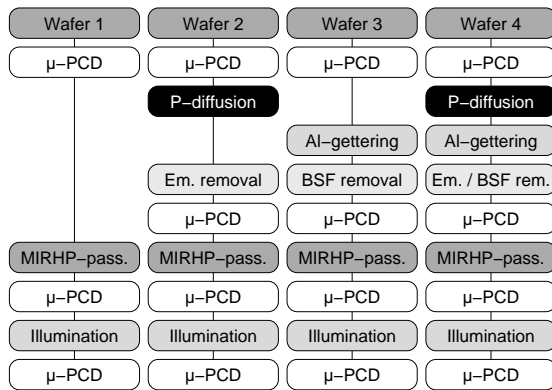


**Figure 1:** Structure of the experiment. After various successive processing steps spatially resolved bulk lifetime measurements have been performed.

### 3 RESULTS

Each time a  $\mu$ -PCD measurement is indicated in Fig. 1, several measurements were performed and combined as described in section 2.1, so that the obtained mappings are reliable in regions of very high lifetime as well as in those of rather low bulk lifetime values. A comparison of the results had shown that lifetime enhancements vary strongly throughout the sample, as it can be seen if mapping (a) of Fig. 2 is compared to (e) for example. As one might assume that areas improve the more the higher the starting lifetime is, the first mapping of each wafer has been split into three “sub-mappings” according to the starting lifetimes. In the following the lifetime changes in these sub-mappings caused by the different processing steps have been visualised in order to examine the correctness of the mentioned assumption. The results of wafer 2 are shown in Fig. 2 representatively. Looking at this figure it should be kept in mind that the uniform mid-grey regions appearing in the split sub-mappings do not represent data of points of measurement, but regions where the starting lifetimes have not been within the lifetime range specified for this column of sub-mappings. The measurement data once located there is consequently given in another column. Due to the restriction of grey-scaled images this aspect might be not visible too clearly.

#### 3.1 Split mappings of wafer 2

The lifetime mapping of wafer 2 performed before the application of processing steps has been split up into three sub-mappings as shown in Fig. 2. One with lifetimes of up to  $2\mu\text{s}$  (a1), one with values between 2 and  $7\mu\text{s}$  (a2) and a final one covering lifetimes above  $7\mu\text{s}$  (a3). The corresponding columns (a1)...(d1) etc. illustrate the influences of processing steps on the areas of each lifetime range. Mappings (ax) show the starting lifetimes whereas (bx), (cx) and (dx) give the gain or losses achieved by the different processing

steps related to the lifetimes measured before the individual step. Graph (c1), for example, shows the difference between lifetimes after hydrogen passivation and those after P-gettering for those areas which had a starting lifetime of up to  $2\mu\text{s}$ . Mapping (e) finally illustrates the final lifetime values reached after completion of wafer 2's processing sequence shown in Fig. 1.

Looking at the alterations caused by P-gettering and in this case at the histograms of mappings (b1) to (b3) it seems as if the assumption of a more efficient lifetime enhancement of regions with higher starting lifetimes mentioned above is correct. The regions of starting lifetimes of up to  $2\mu\text{s}$  in (b1) are only insufficiently enhanced by a few microseconds or in the best case about  $10\mu\text{s}$ . In the second column, or histogram of mapping (b2) respectively, improvements have been stronger. And the highest lifetime gains of about  $120\mu\text{s}$  have been found in a region with a starting lifetime above  $7\mu\text{s}$ . But the assumption turns out to be wrong if the mappings are consulted. There it can be clearly seen that regions of comparable starting lifetime can react very differently on processing steps. In the case of P-gettering, for example in picture (b3), areas with lifetime enhancements of hundred or more microseconds are found as well as such which have just improved by  $30$  to  $50\mu\text{s}$ . Similar regions occur in all mappings of row (bx).

Such effects are visible even more striking in sub-mappings after hydrogen passivation (cx). In each of the mappings regions can be found in which the lifetime alterations caused by MIRHP passivation differ by up to  $100\mu\text{s}$ . For illustration reasons areas have been marked in each category which show the same starting lifetime but react differently on the applied processing steps so that the final lifetime values in (e) are strongly different.

With respect to solar cell fabrication, however, the different reactions of regions with a starting lifetime above  $7\mu\text{s}$  seem to be less important as in this case nearly all points show a final lifetime of more than  $30\mu\text{s}$ . In the cases of lower starting lifetime instead, cell efficiency might be limited by regions which are not sufficiently improved by gettering and passivation techniques. This is the case for the one marked by the right ellipse which has hardly improved during the different processing steps.

Moreover, due to the existence of such regions of different behaviour integral lifetime measurements seem not to be well suited for a precise analysis of String Ribbon silicon material as those areas are inhomogeneously distributed according to usual wafer sizes. The nature of regions incorporated in an examined sample as well as their share of the whole wafer strongly influences the results of the measurements. Consequently, spatially resolved measurement techniques should be used for detailed lifetime investigations instead.

MIRHP passivation of wafer 2 has turned out to be quite stable at least in the case of starting lifetimes of up to  $7\mu\text{s}$ . The differences in lifetime values between the mappings before and after illumination given in (d1) and (d2) of Fig. 2 have to be related to the absolute values given in (e) so that they are in the range of measurement accuracy. In regions of starting lifetimes above  $7\mu\text{s}$ , however, bulk lifetimes tend to decrease a bit during illumination, especially in areas of very high lifetimes. But again the changes have to be related to the absolute lifetimes given in (e). Doing so, a decrease of

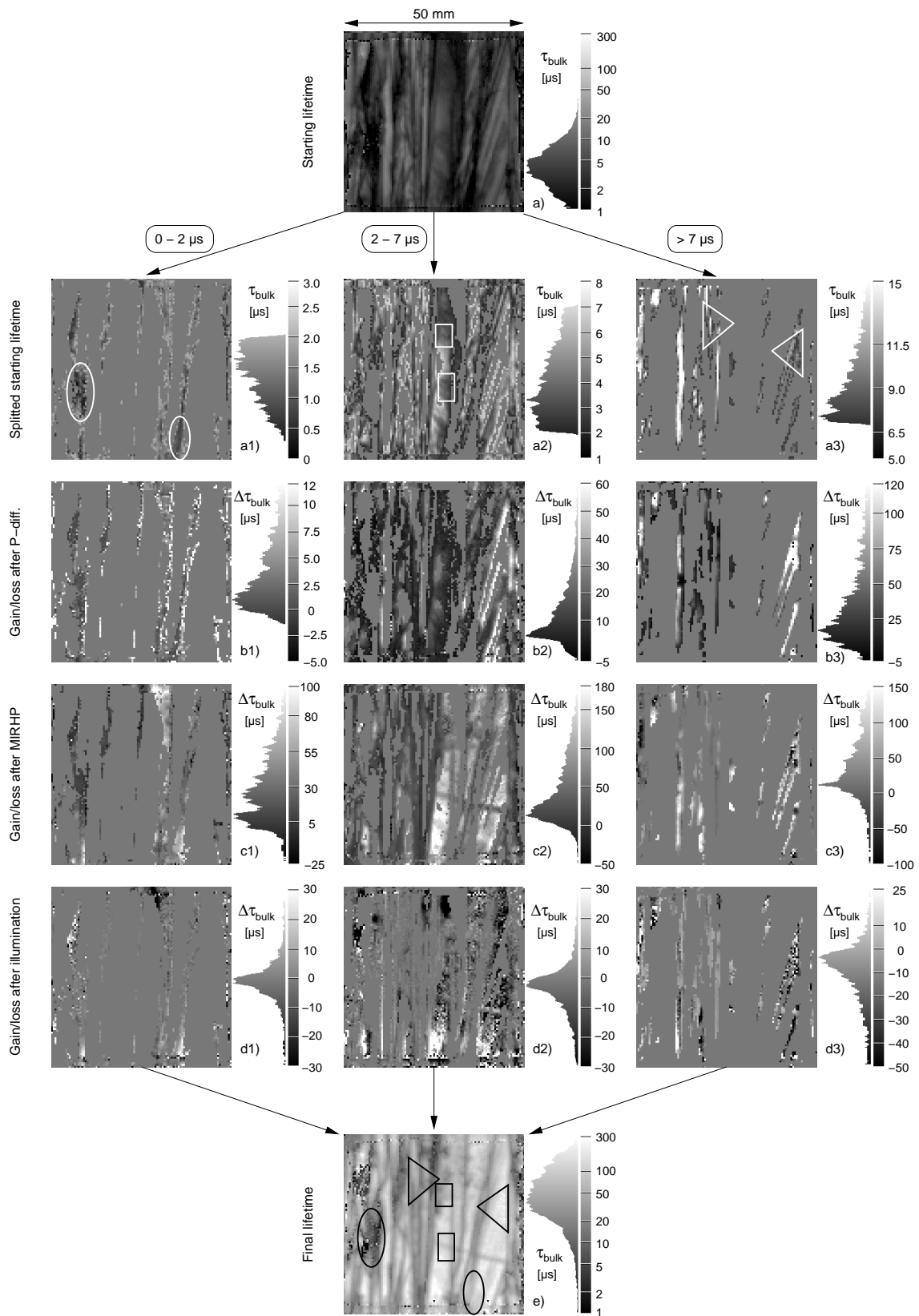


**Figure 2:** Bulk lifetime mappings of wafer 2 as obtained after appropriate combination of various measurements that lead to reliable high and low lifetime values. Mappings have been split according to their starting lifetimes. Graphs (a), (ax) and (e) show absolute lifetime values, whereas (bx), (cx) and (dx) illustrate gains or losses caused by each processing step as related to the lifetime values measured before this individual step.

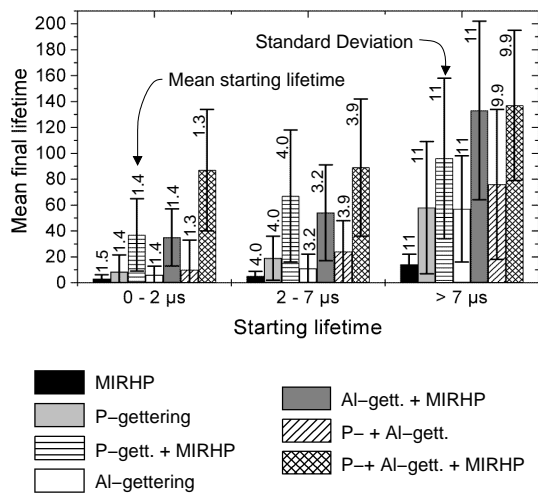


**Figure 3:** Mean final lifetime values after different processing steps (see Fig. 1) calculated for regions of different starting lifetimes.

40 $\mu$ s in regions with absolute bulk lifetimes of 250–300 $\mu$ s appears less severe. Firstly, because the measurement is not more accurate than 10%, and secondly, because a decrease of this extent does not limit the efficiency of conventional solar cells if starting lifetimes are as high as in this case.

### 3.2 Comparing processing steps

In order to compare the impact of different processing steps the mappings belonging to the differently treated wafers of Fig. 1 have been split into three groups of different starting lifetimes as explained in the previous section for the case of wafer 2. In the following mean lifetime values for the various sub-mappings have been calculated which are shown in Fig. 3 together with the mean starting lifetime of the different sub-mappings of each sample. The results look similar to those known from integral measurements. But looking at the very large standard deviation it becomes clear that an enormous amount of information has been lost by the calculation of mean values despite of the fact that the measurements have already been split into groups of different starting lifetimes. Nevertheless some information can be gained from this graph. So for lifetimes below 2 $\mu$ s P-gettering followed by Al-gettering and a subsequent MIHRP passivation step seems to be more efficient than P-gettering or Al-gettering followed by hydrogenation. In the case of higher starting lifetimes, instead, deviations are too large for a conclusion. Consequently, further information can only be provided by the analysis of mappings. An entirely clearly visible aspect, however, is that MIRHP passivation is much less efficient if no gettering step precedes hydrogenation. In this connection it does not matter if P- or Al-gettering or both is performed.

### SUMMARY

It has been shown in this study that in areas with starting lifetimes below 2 $\mu$ s P-gettering followed by Al-gettering and a microwave induced remote hydrogen plasma passiva-

tion is more efficient than P-gettering or Al-gettering followed by a remote plasma hydrogenation step. Furthermore, the applied MIRHP passivation has revealed to have a much less beneficial influence if no gettering step precedes hydrogenation, whereas it does not matter if a P- or Al-gettering or both is performed.

Spatially resolved lifetime measurements have shown strong variations of minority charge carrier bulk lifetimes within some square centimeters of wafer area which become even more striking after gettering and passivation. Additionally, it has been found that there exist regions of comparable starting lifetimes within String Ribbon silicon which are affected to different extents by various solar cell processing steps. Some improve very strongly reaching lifetimes of up to 300 $\mu$ s whereas others are only insufficiently enhanced. Moreover, these areas of different behaviour seem to be inhomogeneously distributed according to usual wafer sizes. As a consequence integral lifetime measurement techniques are influenced by their existence. Therefore, spatially resolved measurement techniques are required for detailed analyses of String Ribbon silicon material.

### ACKNOWLEDGEMENT

The authors gratefully acknowledge the technical assistance of M. Keil during furnace processes.

### REFERENCES

- [1] A. Rohatgi, V. Yelundur, J. Jeong, A. Ebong, D. Meier, A. M. Gabor, M. D. Rosenblum, Proc. 16th EC PVSEC, Glasgow, UK (2000) 1120.
- [2] V. Yelundur, A. Rohatgi, J-W. Jeong, A. M. Gabor, J. I. Hanoka, R. L. Wallace, Proc. 28th IEEE PVSC, Anchorage, Alaska (2000) 91.
- [3] P. Geiger, G. Hahn, P. Fath, E. Bucher, Proc. 16th EC PVSEC, Glasgow, UK (2000) 1214.
- [4] M. Spiegel, P. Fath, K. Peter, B. Buck, G. Willeke, E. Bucher, Proc. 13th EC PVSEC Nice, France (1995) 421.